Nanoscale

COMMUNICATION

View Article Online
View Journal | View Issue

Cite this: *Nanoscale*, 2026, **18**, 9592

Received 22nd May 2025,
Accepted 9th March 2026

DOI: 10.1039/d5nr02175h

rsc.li/nanoscale

Engineering non-linear mechanical advantage in DNA nanostructures: a wireframe adaptation of a lamina emergent mechanism

D. Sebastian Arias [a] and Rebecca E. Taylor *[a,b,c]

Despite significant advances in DNA nanotechnology, dynamic DNA nanostructures have continued to predominantly rely on hinged motion with linear mechanical responses as achieving more sophisticated non-linear mechanical behaviors presents significant challenges. Here, we present a DNA origami lever with a non-linear mechanical advantage that is adapted from a lamina emergent mechanism. The macroscale compliant mechanism is adapted to a wireframe DNA origami structure through strategic bundle placement and single-stranded DNA joints. This structure presents a variable mechanical advantage across its range of motion, where input displacements at the handle produce amplified displacements at the jaws. The kinematics of the structure emerge from its spatial configuration rather than from the design of its joints. Through this adaptation, we show that geometric constraints and spatial relationships can generate complex motion while maintaining relative structural simplicity. This approach represents a paradigm shift in DNA structural design, demonstrating a new avenue for achieving sophisticated mechanical behaviors through geometric configurations rather than complex joint design or through hierarchical arrangement of multiple mechanical components with coordinated behaviors. Moreover, it presents a roadmap for the future adaptation of such systems.

Introduction

Although the DNA origami technique allows for the design of vastly complex mechanisms, a majority of structures that have been utilized in the field are static and often tile and brick-like structures. These stable, well-defined structures have served as versatile tools to explore a wide array of systems from cellular mechanics to photonics, particularly when serving as a "breadboard" to precisely place nanoparticles.[1–8] However, their inherent static design can preclude them from being applied in scenarios that require responsive or adaptive behavior such as active biosensing, targeted drug delivery, and smart materials which respond to environmental stimuli. For these applications, the ability to design dynamic DNA origami nanostructures has been pivotal and has allowed an increased scope of potential applications.[9–12]

Still, the dynamic designs that have been demonstrated in the field remain fairly simple with a predominance of linear hinged motion. The linearity of these systems has considerable limitations. First and foremost they have a restricted range of motion with limited amplification capabilities. Moreover, their linearity imposes a proportionality between size and mechanical output, a drawback which is particularly important due to the size limitations imposed by the scaffold length. As a result, their responsive sensing capabilities can be limited. More broadly, these simple dynamics pale in comparison with the sophisticated non-linear mechanical behaviors exhibited by biological molecular machines. For example, motor proteins like kinesins and myosins achieve remarkable efficiency and force through non-linear force–displacement relationships in their conformational dynamics that enable complex mechanical functions at the nanoscale despite size and energy constraints.[13]

Moving towards structural designs that exhibit complex nonlinear motion represents a fundamental paradigm shift in DNA origami mechanics, not merely an incremental improvement over existing designs. The facile and robust implementation of non-linear mechanical advantage in DNA nanostructures could enable several previously unattainable applications. For instance, in biosensing, the amplification behavior could convert sub-nanometer conformational changes (below the detection threshold of techniques like FRET) into larger displacements within optimal detection ranges. Similarly, in nanorobotics, non-linear levers could create precise mechanical logic gates where small input forces are selectively amplified only when they exceed specific thresholds

[a]*Department of Mechanical Engineering, Carnegie Mellon University, Pittsburgh, Pennsylvania 15213, USA. E-mail: bex@andrew.cmu.edu*
[b]*Department of Biomedical Engineering, Carnegie Mellon University, Pittsburgh, Pennsylvania 15213, USA*
[c]*Department of Electrical and Computer Engineering, Carnegie Mellon University, Pittsburgh, Pennsylvania 15213, USA*

enabling mechanical computation. These capabilities would represent significant advances beyond what is possible with current linear DNA mechanical systems. More broadly, such non-linear behaviors would begin to bridge the sophistication gap between our synthetic DNA machines and the complex mechanical functions exhibited by biological systems.

Previous efforts to create more sophisticated DNA mechanical systems have made important contributions through approaches that combine multiple linear mechanisms or implement specialized joint designs.[9,14] While these approaches have yielded valuable insights into of complex functional structures, they often face significant challenges with the design and implementation. The extreme difficulty involved in engineering precise joints and assembling multiple components into coherent functional systems presents a substantial barrier to adoption and application. Our work seeks to complement these approaches by exploring alternative design principles that can achieve complex mechanical behaviors though simpler means.

Herein we take a look at the implementation of a different class of device: lamina emergent mechanisms.[15,16] These are a subset of compliant mechanisms that can be fabricated on a plane yet, distinctly, exhibit motion that emerges out of the fabrication plane. Their ability to achieve complex non-linear behaviors by using simple geometric components poses an attractive alternative for achieving DNA nanostructures that exhibit complex behaviors. Moreover, these mechanisms confer two key benefits: for one, their compliant structure can be more readily replicated with the typical use of rigid DNA bundles interconnected with ssDNA that replicate the flexible joints of the device. Secondly, the fact that they can be manufactured on a plane presents a markedly reduced complexity in design when compared to the 3D design that could otherwise be needed. Inspired by these principles, we have developed and characterized a DNA origami lever based on a lamina emergent mechanism that achieves non-linear behavior with, comparatively, minimal structural complexity. Our adaptation from solid-plate designs to DNA-compatible wireframe structures represents a significant technical contribution, creating a translation framework that could potentially be applied to other complex mechanical systems structures. The adoption of lamina emergent mechanisms represents a breakthrough approach that achieves complex non-linear mechanisms through geometric design principles rather than through increased structural complexity.

Original Oriceps design and theory

Lamina emergent mechanisms represent a unique class of compliant mechanisms that are fabricated in a planar configuration yet exhibit motion that extends out of their fabrication plane. This characteristic has made them particularly valuable for applications requiring compact storage and deployment.[15,16] Their ability to transform simple planar structures into complex 3D mechanical systems makes them particularly attractive for molecular-scale designs.

The Oriceps mechanism, originally developed by Edmondson *et al.* is a perfect example of this design approach.[17] Inspired by a children's paper origami toy design named "Chomper", Oriceps was engineered as a compliant forceps design composed of six rigid plates interconnected by flexible regions and designed as a replacement to traditional surgical forceps, see Fig. 1(a and b). Like conventional forceps, when actuated by applying force to the handles, the device produces corresponding movement at the jaws through an out-of-plane folding motion. Although this device was not originally designed for its dynamic response, what makes this mechanism particularly valuable for our purposes is its inherent non-linear mechanical behavior between handle separation (input) and jaw separation (output). This behavior follows a non-linear curve that creates variable mechanical advantage across its range of motion. Crucially, this complex mechanical behavior emerges purely from geometric relationships rather than from complicated joint structures or material properties.

Its kinematics can be mathematically derived using geometric principles, with the derivation approach detailed in the provided SI and key structural points highlighted in Fig. S1. Reformulations in terms of bundle lengths and base pairs are additionally provided in section S2 for practical implementation. By defining key dimensional parameters, we can establish the analytical relationship between the handle separation H and the jaw separation J:

$$J = \frac{2(\cos(2\alpha)(8ac^2 - aH^2 + bH^2) + aH^2 + 8bc^2 - bH^2)}{8c^2 + H^2\cos(2\alpha) - H^2} \quad (1)$$

where a, b, c represent physical dimensions while α defines the angle of the midsection plates (Fig. 1(a)). The non-linearity of this behavior emerges from the 3D folding behavior of the structure.

This relationship gives rise to a non-linear mechanical advantage, derived from eqn (1), that varies significantly across its operational range:

$$\text{Ideal Mechanical Advantage} = \frac{dH}{dJ} = \frac{(8c^2 + H^2\cos(2\alpha) - H^2)^2}{32ac^2H\sin^2(2\alpha)} \quad (2)$$

Notably, the mechanical advantage directly describes force transmission: forces applied at the handle are transmitted to the jaw with a force ratio given by the mechanical advantage. This relationship means that the device exhibits non-linear force transmission characteristics that vary across its operational range. For sensing and actuation applications, the inverse relationship, the displacement amplification, is often more relevant, as it describes how input displacements are magnified at the output:

$$\text{Displacement Amplification} = \frac{dJ}{dH} = \frac{32ac^2H\sin^2(2\alpha)}{(8c^2 + H^2\cos(2\alpha) - H^2)^2} \quad (3)$$

Several important insights emerge from these equations. First, the amplification is directly proportional to dimension a

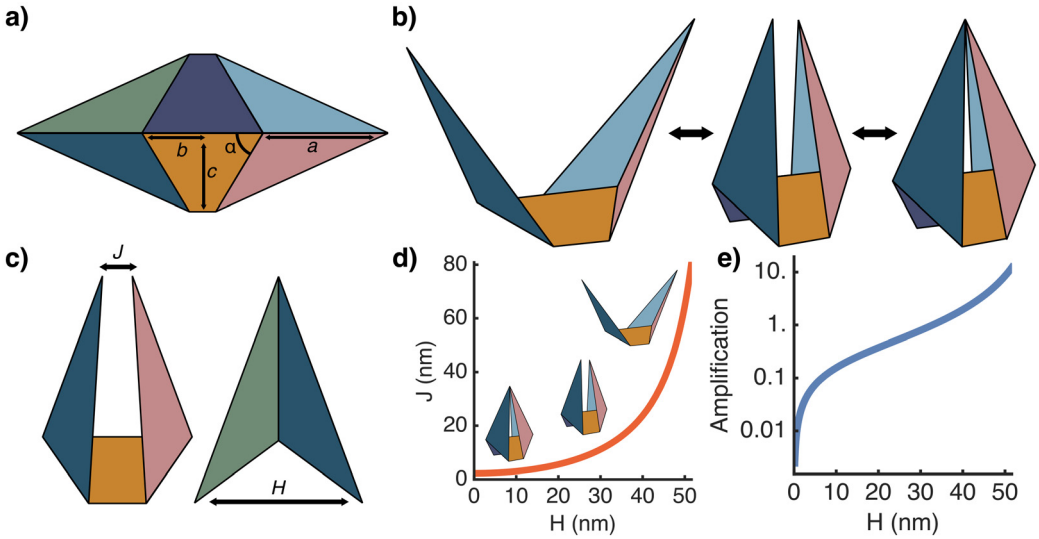

Fig. 1 (a) Original Oriceps design shown with key dimensional parameters that define its geometric properties. (b) Depiction of the progression of the structure from open to closed positions, illustrating the out-of-plane motion. (c) Side and front views of the device with jaw Separation J and handle separation H highlighted. (d) Analytical jaw–handle relationship with a = 26.2 nm, b = 14.2 nm, c = 25.8 nm, and α = 60°. Curve demonstrates characteristic non-linear behavior. (e) Resulting amplification ratio between the jaw and handle displacements, showing how the mechanical advantage varies with handle separation.

(the length of the jaw), making this a potentially easily tunable parameter for optimizing or modulating amplification. Second, the $\sin^2(2\alpha)$ and $\cos^2(2\alpha)$ terms indicate that the amplification is highly sensitive to the midsection angle. Moreover, as H approaches zero (closed handles), the amplification approaches zero. Lastly, the amplification is independent of the value of b.

Fig. 1(d and e) illustrates one such behavior. The non-linear J–H curve and its corresponding amplification show how the structure transforms input displacements at variable rates across its range of motion. Importantly, this kinematic behavior is highly tunable through simple geometric adjustments, making the structure remarkably versatile as designers can tailor the response curve to specific applications without altering fundamental design principles.

DNA origami adaptation and design approach

While this mechanism offers an elegant framework for achieving non-linear mechanical advantages, there are multiple challenges in translating a solid-plate macroscale design into a DNA origami structure while preserving the geometric relationships that result in the desired non-linear behavior.

Although a direct replica of the solid plate approach could be feasible, it presents several significant limitations. Single-layer and multi-layer DNA origami are well-established in the field, but their use would consume substantial portions of the scaffold strand without significantly increasing the rigidity of the structure. This is particularly true for single-layer DNA origami sheets which exhibit considerable flexibility.[18] Moreover, reproducing the precise angled joints between DNA sheets would require complex edge connections and be heavily limited by the physical constraints of DNA.

Instead, a wireframe version that captures the essential geometric relationships of the Oriceps mechanism while overcoming these limitations is developed. This approach offers two significant advantages: for one, DNA bundles provide substantially higher rigidity than sheets. Secondly, the wireframe approach simplifies joint design, as each vertex can be formed with flexible ssDNA connections that permit rotation without requiring precise angular constraints. This transition to a wireframe structure further necessitates a critical modification: the redesign of the midsection from a trapezoidal to a triangular shape (Fig. 2(a)). Unlike trapezoidal wireframe components which lack sufficient constraints to prevent deformation or collapse, triangular elements are geometrically rigid. Thus, this modification ensures the stability and rigidity of a wireframe adaptation.

Our adapted wireframe DNA origami implementation consists of 11 DNA bundles interconnected by flexible ssDNA linkers, as shown in Fig. 2(b). Each bundle is designed with either a 2 × 2 or a 2 × 3 helix cross-section. The specific dimensions were chosen based on multiple factors including number of connections required at each end, the rigidity of the bundles, or to include desired constraints to the joints. Most joint connections between bundles consist of two ssDNA linkers that function as spherical joints, allowing rotation while maintaining positional constraint (Fig. 2(b)III and IV.1). While this design approach could have been applied uniformly throughout the structure, we opted to strategically modify the

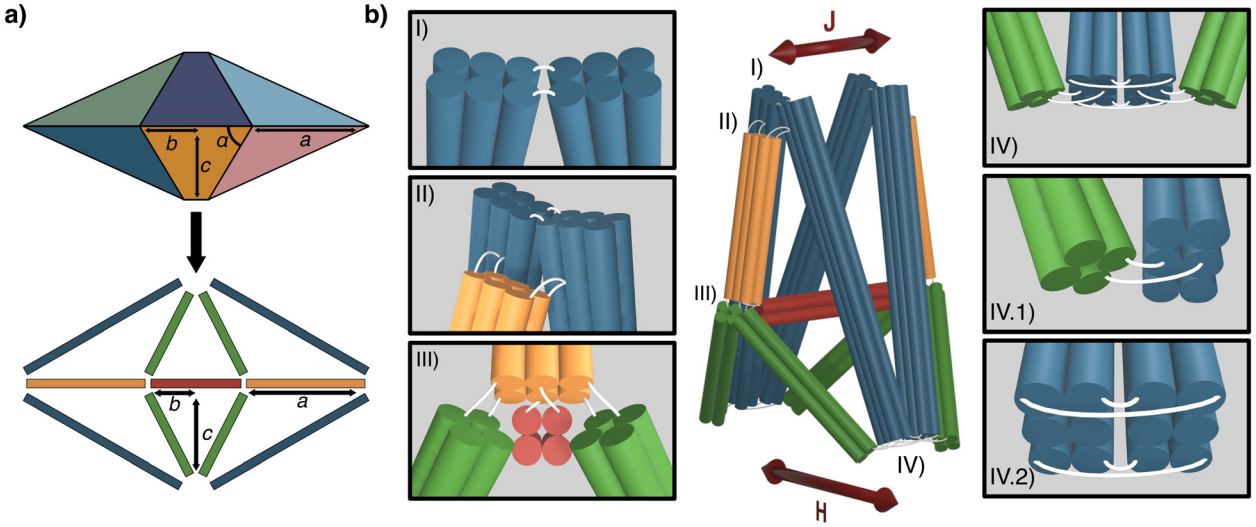

Fig. 2 (a) Conversion from the solid plate Oriceps design (top) to a wireframe implementation (bottom). (b) Visualization of the DNA implementation where dsDNA helices are depicted as solid tubes. Bundles are color-coded by function: jaws (blue), midsection (orange/red), and handles (green). Close-up views of ssDNA connections (white) at different junctions: (I) ssDNA joints at the top of the jaw bundles. (II) Connections between jaw and midsection bundles. (III) Connections between midsection and handle bundles. (IV) Connections between jaw and handle bundles. Separate images are provided for clarity.

jaw bundles to increase functionality. The jaws were designed with a 2 × 3 helix cross-section which allows for increased inner surface area for potential conjugation of functional molecules. The bottom four connection points are placed at the outer edges of the jaw bundles to constrain the closing motion to a single plane, and therefore ensure that the jaws close flat against each other. Additionally, the jaw bundles are slightly extended so that the midsection connections can be positioned towards the backside of the jaw bundles. This creates a bias in the folding direction and thereby prevents unwanted inversion of the structure. This positioning also increases the available surface area for potential functionalization.

To facilitate validation of the mechanical properties of the structure, the unused portion of the scaffold was strategically routed to form a truss that bridges the handles of the device, specifics of the bridge design found in Fig. S3. Its length, and therefore its handle separation, can be easily altered through the use of different staple strands. This design of the bridging truss allows the formation of structures with predetermined handle separations, and is thereby used as an experimental control mechanism during simulation and experimental validation.

Wireframe design mathematical framework

The triangular midsection of our wireframe adaptation simplifies the original behavior (eqn (1)) to the case where $\alpha = \tan\frac{c}{b}$. This eliminates α as a variable and results in an equation that depends solely on the structural dimensions a, b, and c:

$$J = \frac{2a(4b^2 - 4c^2 + H^2) + 8b^3 + 8bc^2 - 2bH^2}{4b^2 + 4c^2 - H^2} \quad (4)$$

This equation, and our wireframe design, preserve the essential non-linear relationship between handle separation H and jaw separation J. As in the original design, this mathematical relationship leads to a non-linear mechanical advantage and corresponding displacement amplification that can similarly be derived from eqn (4):

$$\text{Ideal Mechanical Advantage} = \frac{dH}{dJ} = \frac{(-4b^2 - 4c^2 + H^2)^2}{32ab^2H} \quad (5)$$

$$\text{Displacement Amplification} = \frac{dJ}{dH} = \frac{32ab^2H}{(-4b^2 - 4c^2 + H^2)^2} \quad (6)$$

For any set of dimensions, a, b, and c, the jaw separation J will range from a minimum of $\frac{2(ab^2 - ac^2 + b^3 + bc^2)}{b^2 + c^2}$ when the handles are completely closed ($H = 0$) to a maximum of $2(a + b)$ when the handles are fully opened ($H = 2c$). Its amplification will range from 0 when fully closed to a maximum amplification of $\frac{4ac}{b^2}$ when fully open. Notably, and in contrast with eqn (3), the amplification in this case does depend on b, this is a direct result of the triangular midsection modification, as the effects of α are integrated into b and c.

For the device characterized in this study, we selected dimensions: a = 26.2 nm (77 bp), b = 14.2 nm (42 bp), c = 25.8 nm (76 bp). Although many possible dimensions could have been chosen, these dimensions result in a device whose

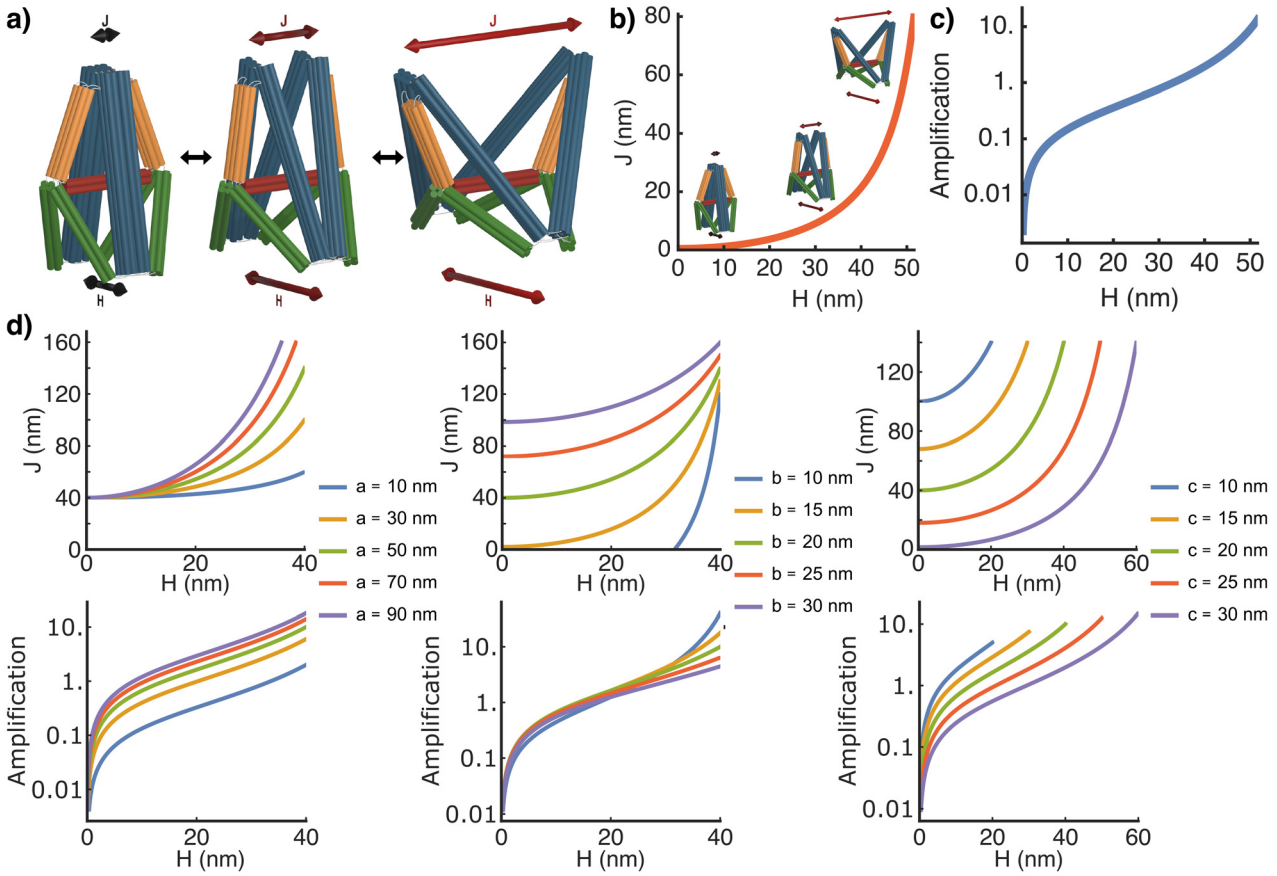

Fig. 3 3D model of wireframe adaptation and its analytical behavior (a) 3D models of the structure at different open configurations. The device behaves like a lever, in which there is a correspondence between the handle separation *H* and the jaw separation *J*. (b) *J*–*H* behavior for our structure with *a* = 26.2 nm (77 bp), *b* = 14.2 nm (42 bp), *c* = 25.8 nm (76 bp). (c) Resulting amplification between displacements at the jaws and handles. (d) Number of different behaviors showcasing the effect of varying the three dimensions, demonstrating the tunability of the device. Corresponding amplification curves are shown below each behavior plot. Other variables held constant at: *a* = 50 nm, *b* = 20 nm, and *c* = 20 nm. Similar plots for the original Oriceps plate design are provided in Fig. S4.

analytical *J*–*H* behavior sweeps out a large range, and provides a good testbed for this first demonstration of non-linear mechanical advantage in DNA origami. The predicted behavior and corresponding amplification are shown in Fig. 3 along with a set of behaviors that demonstrate the effect of varying the three variables to demonstrate the tunability available.

It is important to acknowledge that these analytical equations represent an idealized model that does not account for several non-idealities inherent to real DNA origami structures: the non-negligible bundle thickness alters the effective dimensions, the ssDNA connections have finite lengths that affect joint positioning, and the inherent flexibility of DNA introduces additional compliance throughout the system. For these reasons the real behavior will inevitably deviate from these theoretical predictions. Beyond providing essential guidance in determining dimensions for a device that would cover a targeted behavior, the analytical equations reveal which non-idealities will most significantly affect the device's behavior. The maximum amplification's quadratic dependence on *b* means that compliance and other non-idealities in the midsection bundles will have the largest impact on the realized mechanical advantage. In contrast, *a* and *c* influence the maximum amplification only linearly, making these parameters more tolerant to dimensional variations.

Characterization

To validate our design and characterize its predicted non-linear behavior, we first use the oxDNA coarse-grained molecular dynamics framework.[19–22] This approach has been extensively validated for DNA origami structures and is capable of providing realistic predictions of structural conformation and mechanical behavior. Multiple oxDNA simulations were performed with varying handle constraints to sample the full range of the device's behavior. Fig. 4(a) shows representative configurations from these simulations with handle separations ranging from approximately 10 nm to 50 nm and illustrates how the structure correctly adopts different conformations as the handle separation increases. To quantitatively analyze the

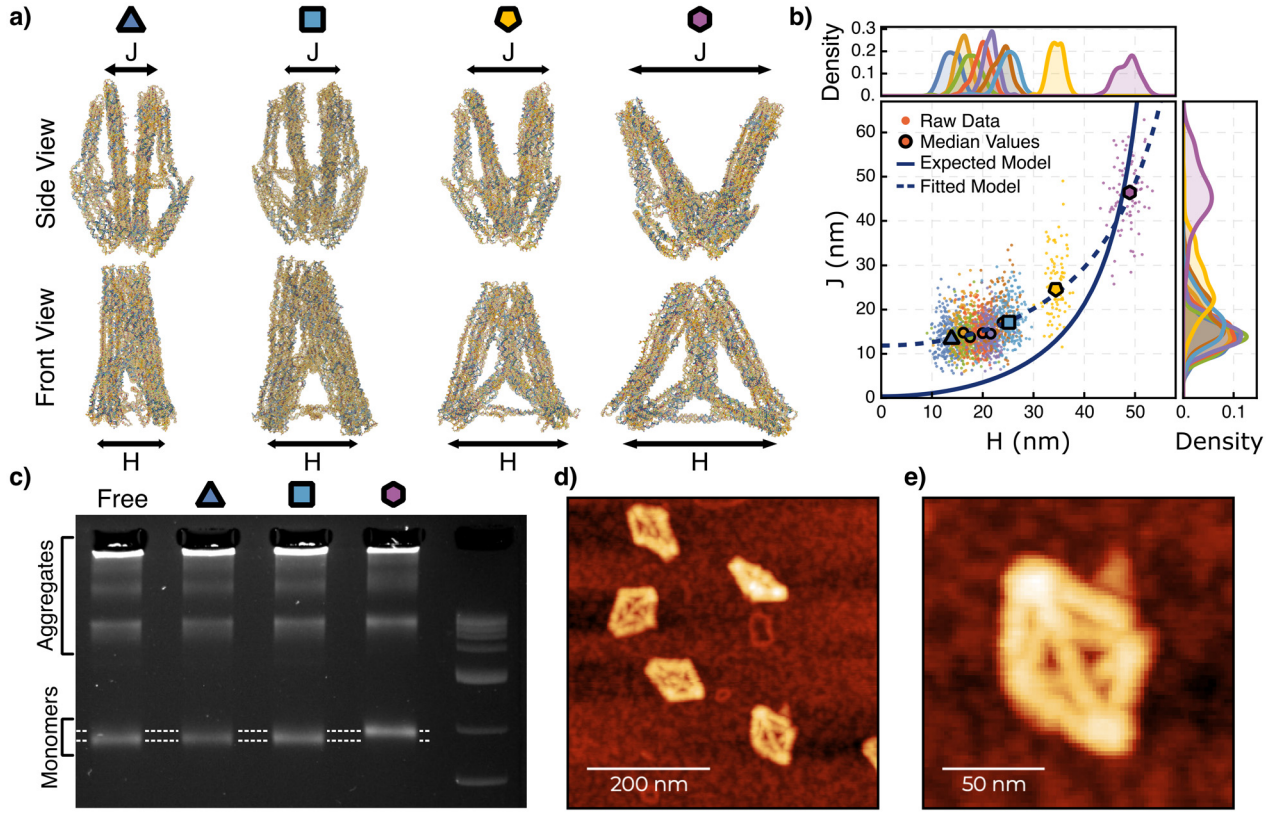

Fig. 4 (a) Centroid configurations from oxDNA simulations showing DNA Oriceps structures with different handle constraints, controlled by strut lengths, resulting in increasing jaw (*J*) and handle (*H*) separations. Side and front views illustrate the 3D conformational changes. Colored circles above each configuration corresponds to the matching data points in panel b. (b) *J*–*H* relationship data from simulations. Main plot shows raw data points (colored dots), corresponding median values (black outlined dots), the expected theoretical model (solid blue line), and the fitted model (dashed blue line). Side plots show density distributions of *J* and *H* measurements. (c) Agarose gel electrophoresis characterization of DNA Oriceps formed with different handle openings, *H*. Colored circles above each configuration corresponds to the matching data points in panels a and b. The band labeled "Free" corresponds to structures where the portion of the scaffold that bridge the handles are left as ssDNA. The last lane corresponds to a gel ladder. (d) AFM images of multiple DNA Oriceps structures deposited on mica after gel electrophoresis band purification. Scale bar: 200 nm. Pre- and post-purification AFM images comparison found in Fig. S6 along with AFM images of other configurations. (e) Higher magnification AFM image of a single DNA Oriceps structure showing detailed wireframe structure. Scale bar: 50 nm.

mechanical behavior, we extracted jaw separation *J* and handle separation *H* measurements across these simulations, with results plotted in Fig. 4(b).

The simulation data clearly demonstrates that our DNA origami lever maintains an expected non-linear behavior, with the jaw separation exhibiting a distinctly non-linear response to increasing handle separations. As expected, however, the simulations reveal significant deviations from the analytical model due to previously noted non-idealities of real DNA origami. Fitting the data to our analytical model gives us effective dimensional parameters of: $a = 34(4)$ nm, $b = 20(1)$ nm, and $c = 30(1)$ nm. These values are notably larger than our design dimensions by approximately 8 nm for a and 5 nm for both b and c. The fit parameters demonstrate good agreement with our model while accounting for the physical dimensions of the DNA origami structure. The increased effective values for b and c align with expectations, as they incorporate both the physical thickness of the DNA bundles and the slack introduced by the ssDNA connections. The larger increase in a reflects not only these effects but also our intentional design choice to extend the jaw bundles beyond their connection points with the midsection.

DNA Oriceps were synthesized and characterized using standard DNA origami approaches.[23] The primary objectives of our experimental characterization were to confirm successful structure formation and to validate the structural configurations predicted by our design and simulations. Agarose gel electrophoresis provided evidence of successful structure formation across all handle configurations, see Fig. 4(c). The gel revealed distinct bands corresponding to monomer structures across all samples, with higher bands corresponding to increasingly aggregated structures. The well-defined monomer bands demonstrating consistent assembly regardless of bridge length. Additionally, the gel provided qualitative evidence of conformational differences between configurations. Structures formed with the largest handle separation constraint, exhibited notably slower gel migration than the cases with smaller handle constraints, all of which ran at similar rates. This

result is consistent with the non-linear behavior that we expect based on the design and our simulation studies, where more open configurations present larger hydrodynamic radii and consequently experience greater drag forces during electrophoresis. However, the relatively modest mobility difference between our most extreme configurations, combined with the inherent structural flexibility evident in our simulations (particularly at higher H values), indicates that gel electrophoresis provides limited resolution for quantitatively mapping the J–H relationship. Interestingly, structures formed without a defined bridge constraint exhibited migration rates consistent with the more compact configurations. This observation suggests that our unconstrained structure adopt a compact conformation, which further aligns with simulation results (individual simulation data plotted in Fig. S5). Still, the observable mobility difference suggests potential applications in gel-based sensing assays, where binding events or conformational changes could produce detectable shifts in band migration. While such applications would require further optimization to enhance resolution and increase mobility deltas, the principle demonstrated here provides a foundation for future development of such readouts.

Atomic force microscopy (AFM) provided direct visual confirmation of successful structure formation at the single-molecule level. As shown in Fig. 4(d and e), AFM imaging revealed structures with the expected wireframe architecture. Higher resolution imaging of individual structures showed all eleven designed bundles in the correct configuration, confirming that our wireframe design successfully translates to physical DNA origami structure.

These results provide strong validation of our DNA origami lever design. The successful formation of the complete wireframe structure demonstrates that lamina emergent mechanism principles can be effectively translated to DNA origami. The migration patterns in agarose gel electrophoresis provide evidence of the mechanical properties of the structure and configurations while AFM imaging validates the structural conformation of the structure. Together, these findings confirm that we have successfully created a DNA origami structure capable of implementing the geometric principles required for non-linear mechanical advantage. Methods for the design,[24,25] synthesis,[23] and computational[26] and experimental characterization are detailed in the provided SI followed by sequence information in Table S1.

Discussion and conclusions

In this work, we have successfully designed, computationally verified, and experimentally formed a DNA origami lever that exhibits non-linear mechanical behavior. By adapting the lamina emergent Oriceps mechanism, we have demonstrated a novel approach for creating complex mechanical systems that go beyond the linear mechanisms that have dominated the field. Our wireframe implementation successfully preserves the essential geometric relationships that give rise to the demonstrated non-linear mechanical advantage while accommodating the design constraints of DNA origami.

The transition from a solid plate design to a wireframe structure represents a substantial design adaptation that effectively balances structural integrity with the material limitations of DNA origami. Our triangular midsection redesign ensures structural stability while the strategic placement of ssDNA connections creates flexible joints that enable the complex 3D motion required for the structure's actuation. Computational simulations confirm that this approach successfully captures the non-linear mechanical advantage inherent to the original design, with deviations that can be attributed to the physical realities of DNA nanostructures. While the geometric relationships are well-preserved, the simulations also reveal significant structural flexibility, particularly at higher handle separations where the structure samples broader conformational distributions. This flexibility would present a significant consideration for force transmission applications, as bundle compliance and joint flexibility would result in force-dependent deformation, affecting the effective mechanical advantage under applied loads. Such considerations would be important for future application-directed development, where structural optimization could enhance rigidity for force-based applications.

Experimental characterization through gel electrophoresis and AFM imaging provides compelling evidence for the successful formation of the structure with the expected configuration. Particularly revealing is the difference in observed migration rates between structures with the different handle separations, which aligns with our theoretical predictions and computational models. This serves as evidence that the DNA origami structure maintains distinct conformational states corresponding to different handle separations. The agreement between theory, simulation, and experiment validates our design approach and demonstrates the feasibility of implementing complex mechanical systems at the nanoscale.

The ability to construct DNA nanostructures with non-linear mechanical advantages represents a significant advancement in structural DNA nanotechnology. While previous work has primarily focused on simple hinged motions with linear response characteristics, our approach demonstrates that more sophisticated mechanical behaviors can be achieved through careful geometric design rather than increased joint complexity or the coupling of multiple coordinated subcomponents. This design philosophy of achieving functional complexity through geometric constraints and spatial relationships rather than through elaborate structural design could prove valuable for addressing other challenges in DNA nanotechnology.

The non-linear relationship between input and output displacements offers several potential advantages for nanoscale applications. Most importantly, this non-linearity enables the decoupling of mechanical output from structural size, allowing for the design of compact devices with enhanced mechanical performance. With appropriate structural optimization and integration of functional elements sensing applications based on this design principle could potentially improve signal-to-

noise ratios by transforming small input signals into larger, more easily detected displacements, enabling the detection of smaller stimuli that would be undetectable with conventional linear mechanisms. Realizing such applications would require addressing the structural flexibility observed in the current design, integrating molecular recognition elements, and developing appropriate readout mechanisms, each of which represents an important direction for future work.

More broadly, this work provides a proof-of-concept demonstration of how lamina emergent mechanisms can be successfully translated to DNA origami nanostructures. By identifying and preserving the essential geometric relationships while accommodating DNA origami design constraints, we've established a methodology that could be applied to other lamina emergent mechanisms. The structural modifications, strategic placement of ssDNA joints, and bundle implementation of structural elements represent key principles that could guide the adaptation of more complex mechanisms. Application-directed development will require reducing thermal fluctuations through optimized bundle dimensions and joint placements, exploring different dimensional parameters to tailor the mechanical response curves for specific applications, along with integration of the functional elements necessary for each application domain.

Beyond this initial implementation of Oriceps, the broader exploration of other lamina emergent mechanisms presents particularly exciting opportunities. The mechanical engineering literature offers a rich variety of lamina emergent systems with diverse behaviors that could be adapted using the design principles established here. With appropriate development and optimization, expanding this exploration could lead to sophisticated nanoscale machines that perform complex mechanical operations previously unattainable with DNA nanotechnology. These developments, combined with DNA's programmability and biocompatibility, may enable transformative applications in molecular sensing, targeted drug delivery, and synthetic cellular systems where precisely controlled mechanical behaviors could significantly enhance functionality.

Author contributions

D. S. A. performed the formal analysis, investigation, methodology development, software implementation, validation, and visualization, and wrote the original draft. R. E. T. acquired funding, provided project administration and supervision. Both authors contributed to conceptualization and participated in review and editing of the manuscript. All authors have read and approved the final version of the manuscript. Author contributions follow the CRediT (Contributor Roles Taxonomy) framework.

Conflicts of interest

There are no conflicts of interest to declare.

Data availability

The data supporting this article have been included as part of the supplementary information (SI) including analytical model derivations, simulation data, design file renders, and DNA sequences. Supplementary information is available. See DOI: https://doi.org/10.1039/d5nr02175h.

Acknowledgements

This work was supported in part by the Air Force Office of Scientific Research DURIP FA9550-22-1-0147 and YIP FA9550-18-1-0199, as well as the National Science Foundation ECCS #2132886.

References

1 Y. Suzuki, M. Endo, Y. Katsuda, K. Ou, K. Hidaka and H. Sugiyama, DNA Origami Based Visualization System for Studying Site-Specific Recombination Events, *J. Am. Chem. Soc.*, 2014, **136**, 211–218.
2 A. Shaw, V. Lundin, E. Petrova, F. Fördős, E. Benson, A. Al-Amin, A. Herland, A. Blokzijl, B. Högberg and A. I. Teixeira, Spatial Control of Membrane Receptor Function Using Ligand Nanocalipers, *Nat. Methods*, 2014, **11**, 841–846.
3 A. Shaw, I. T. Hoffecker, I. Smyrlaki, J. Rosa, A. Grevys, D. Bratlie, I. Sandlie, T. E. Michaelsen, J. T. Andersen and B. Högberg, Binding to Nanopatterned Antigens Is Dominated by the Spatial Tolerance of Antibodies, *Nat. Nanotechnol.*, 2019, **14**, 184–190.
4 P. Wijesekara, Y. Liu, W. Wang, E. K. Johnston, M. L. G. Sullivan, R. E. Taylor and X. Ren, Accessing and Assessing the Cell-Surface Glycocalyx Using DNA Origami, *Nano Lett.*, 2021, **21**, 4765–4773.
5 M. Wang, D. Yang, Q. Lu, L. Liu, Z. Cai, Y. Wang, H.-H. Wang, P. Wang and Z. Nie, Spatially Reprogramed Receptor Organization to Switch Cell Behavior Using a DNA Origami-Templated Aptamer Nanoarray, *Nano Lett.*, 2022, **22**, 8445–8454.
6 V. V. Thacker, L. O. Herrmann, D. O. Sigle, T. Zhang, T. Liedl, J. J. Baumberg and U. F. Keyser, DNA Origami Based Assembly of Gold Nanoparticle Dimers for Surface-Enhanced Raman Scattering, *Nat. Commun.*, 2014, **5**, 3448.
7 G. P. Acuna, M. Bucher, I. H. Stein, C. Steinhauer, A. Kuzyk, P. Holzmeister, R. Schreiber, A. Moroz, F. D. Stefani, T. Liedl, F. C. Simmel and P. Tinnefeld, Distance Dependence of Single-Fluorophore Quenching by Gold Nanoparticles Studied on DNA Origami, *ACS Nano*, 2012, **6**, 3189–3195.
8 P. C. Nickels, B. Wünsch, P. Holzmeister, W. Bae, L. M. Kneer, D. Grohmann, P. Tinnefeld and T. Liedl, Molecular Force Spectroscopy with a DNA Origami–Based Nanoscopic Force Clamp, *Science*, 2016, **354**, 305–307.

9 M. DeLuca, Z. Shi, C. E. Castro and G. Arya, Dynamic DNA Nanotechnology: Toward Functional Nanoscale Devices, *Nanoscale Horiz.*, 2020, **5**, 182–201.
10 S. M. Douglas, I. Bachelet and G. M. Church, A Logic-Gated Nanorobot for Targeted Transport of Molecular Payloads, *Science*, 2012, **335**, 831–834.
11 Y. Wang, J. V. Le, K. Crocker, M. A. Darcy, P. D. Halley, D. Zhao, N. Andrioff, C. Croy, M. G. Poirier, R. Bundschuh and C. E. Castro, A Nanoscale DNA Force Spectrometer Capable of Applying Tension and Compression on Biomolecules, *Nucleic Acids Res.*, 2021, **49**, 8987–8999.
12 J. V. Le, Y. Luo, M. A. Darcy, C. R. Lucas, M. F. Goodwin, M. G. Poirier and C. E. Castro, Probing Nucleosome Stability with a DNA Origami Nanocaliper, *ACS Nano*, 2016, **10**, 7073–7084.
13 Y. Togashi, T. Yanagida and A. S. Mikhailov, Nonlinearity of Mechanochemical Motions in Motor Proteins, *PLoS Comput. Biol.*, 2010, **6**, e1000814.
14 A. E. Marras, L. Zhou, H.-J. Su and C. E. Castro, Programmable Motion of DNA Origami Mechanisms, *Proc. Natl. Acad. Sci. U. S. A.*, 2015, **112**, 713–718.
15 J. O. Jacobsen, B. G. Winder, L. L. Howell and S. P. Magleby, Lamina Emergent Mechanisms and Their Basic Elements, *J. Mech. Robot.*, 2010, **2**, 011003.
16 J. Jacobsen, *Fundamental Components for Lamina Emergent Mechanisms*, Theses and Dissertations, 2008.
17 B. J. Edmondson, L. A. Bowen, C. L. Grames, S. P. Magleby, L. L. Howell and T. C. Bateman, in *ASME 2013 Conference on Smart Materials, Adaptive Structures and Intelligent Systems*, 2014.
18 M. A. B. Baker, A. J. Tuckwell, J. F. Berengut, J. Bath, F. Benn, A. P. Duff, A. E. Whitten, K. E. Dunn, R. M. Hynson, A. J. Turberfield and L. K. Lee, Dimensions and Global Twist of Single-Layer DNA Origami Measured by Small-Angle X-ray Scattering, *ACS Nano*, 2018, **12**, 5791–5799.
19 P. Šulc, F. Romano, T. E. Ouldridge, L. Rovigatti, J. P. K. Doye and A. A. Louis, Sequence-Dependent Thermodynamics of a Coarse-Grained DNA Model, *J. Chem. Phys.*, 2012, **137**, 135101.
20 E. Poppleton, M. Matthies, D. Mandal, F. Romano, P. Šulc and L. Rovigatti, oxDNA: Coarse-Grained Simulations of Nucleic Acids Made Simple, *J. Open Source Softw.*, 2023, **8**, 4693.
21 L. Rovigatti, P. Šulc, I. Z. Reguly and F. Romano, A Comparison between Parallelization Approaches in Molecular Dynamics Simulations on GPUs, *J. Comput. Chem.*, 2015, **36**, 1–8.
22 E. Poppleton, R. Romero, A. Mallya, L. Rovigatti and P. Šulc, OxDNA.Org: A Public Webserver for Coarse-Grained Simulations of DNA and RNA Nanostructures, *Nucleic Acids Res.*, 2021, **49**, W491–W498.
23 K. F. Wagenbauer, F. A. S. Engelhardt, E. Stahl, V. K. Hechtl, P. Stömmer, F. Seebacher, L. Meregalli, P. Ketterer, T. Gerling and H. Dietz, How We Make DNA Origami, *ChemBioChem*, 2017, **18**, 1873–1885.
24 C.-M. Huang, A. Kucinic, J. A. Johnson, H.-J. Su and C. E. Castro, Integrated Computer-Aided Engineering and Design for DNA Assemblies, *Nat. Mater.*, 2021, **20**, 1264–1271.
25 S. M. Douglas, A. H. Marblestone, S. Teerapittayanon, A. Vazquez, G. M. Church and W. M. Shih, Rapid Prototyping of 3D DNA-origami Shapes with caDNAno, *Nucleic Acids Res.*, 2009, **37**, 5001–5006.
26 J. P. K. Doye, H. Fowler, D. Prešern, J. Bohlin, L. Rovigatti, F. Romano, P. Šulc, C. K. Wong, A. A. Louis, J. S. Schreck, M. C. Engel, M. Matthies, E. Benson, E. Poppleton and B. E. K. Snodin, *DNA and RNA Origami: Methods and Protocols*, Springer US, New York, NY, 2023, pp. 93–112.